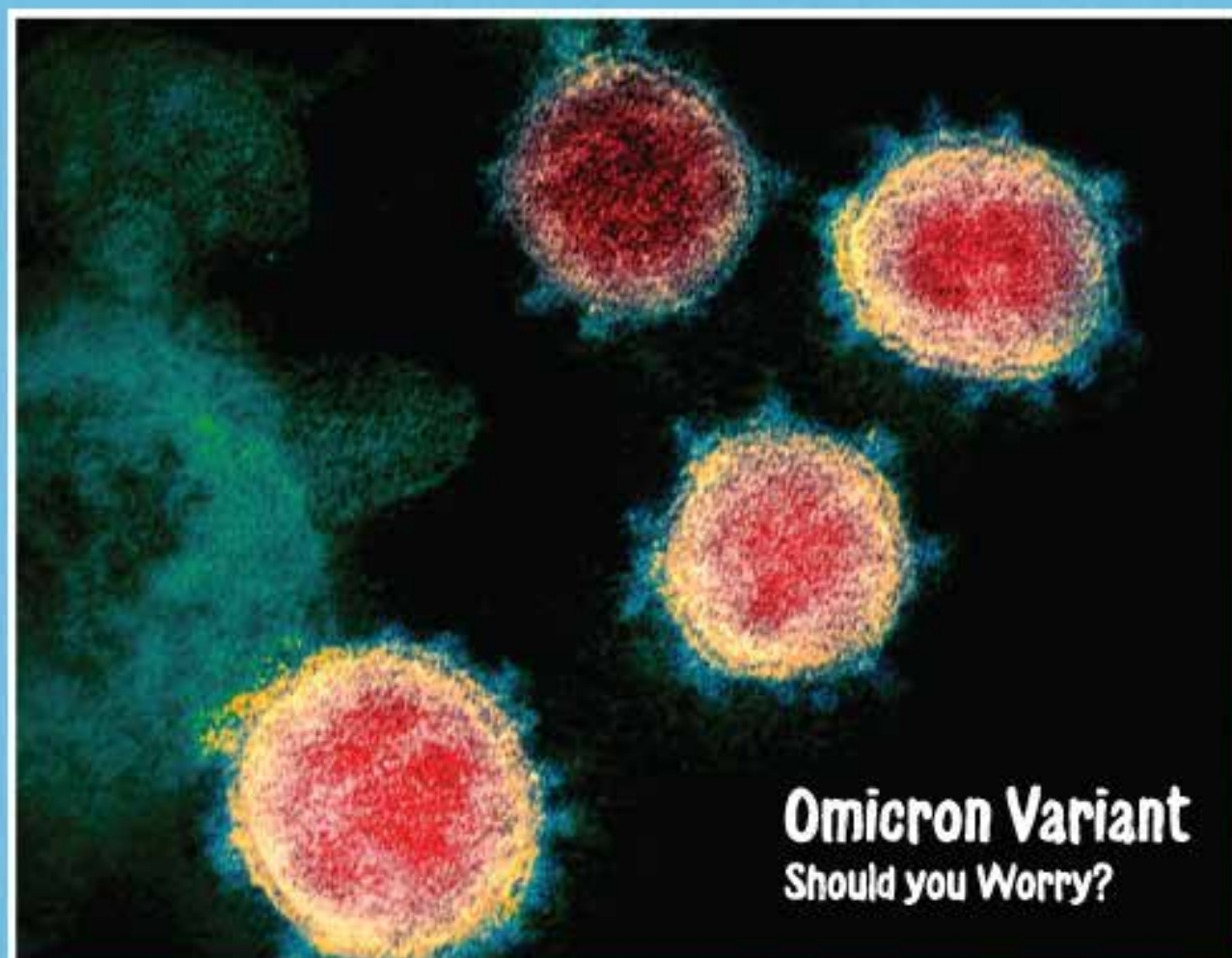


# The Gulf Journal of Oncology



Indexed By PubMed and Medline Database

Issue 38, January 2022  
ISSN No. 2078-2101



**Omicron Variant**  
**Should you Worry?**

The Official Journal of the Gulf Federation For Cancer Control

# Table of Contents

## Original Articles

<b>Image-Guided Brachytherapy a Comparison Between 192Ir and 60Co Sources in Carcinoma Uterine Cervix</b> .....	07
Mourougan Sinnatamby, Saravanan Kandasamy, Gunaseelan Karunanidhi, Vijayaprabhu Neelakandan, Seenisamy Ramapandian, Muniyappan Kannan, Elakiya Sampath	
<b>Immunohistochemical Analysis of Novel Biomarkers Cyclin D1, p53 And Ki67 in Endometrial Carcinoma: Clinicopathological Significance and Prognostic Value</b> .....	15
Manisha A. Atram, V B Shivkumar, Nitin M. Gangane	
<b>Serum Alkaline Phosphatase in Newly Diagnosed Genito-Urinary Cancers – Do We Need to Review the Guidelines?</b> .....	24
Rathee Ravish, Punatar Chirag B, Agrawal Gaurav, Nagaonkar Santoshi, Joshi Vinod S, Late Sagade Sharad N, Srinivas V	
<b>Post-Menopausal Status and Risk for Cervical Dysplasia</b> .....	31
Kenia Edwards, Mary Fatehi, Joshua Fogel	
<b>Impact of Screening Programs on Stage Migration in Breast Cancer</b> .....	38
Bassim Jaffar Al Bahrani, Itrat Mehdi, Taha Mohsin Al Lawati, Abdulaziz M Al Farsi, Najla A. Al Lawati, Hasina Al Harthi	
<b>Assessment of Voice Outcomes Post Chemo-Radiotherapy in Non-Laryngeal Head &amp; Neck Cancers Using Electroglottography and Voice Symptom Scale (VoISS) Questionnaire</b> .....	47
Nikhila Radhakrishna, B. K. Yamini, Amrut Sadashiv Kadam, N. Shivashankar, Chendil Vishwanathan, Rajesh Javarappa	
<b>Predictive and Prognostic Value of Tumor-Infiltrating Lymphocytes for Pathological Response to Neoadjuvant Chemotherapy in Triple Negative Breast Cancer</b> .....	53
Amrallah A. Mohammed, Fifi Mostafa Elsayed, Mohammed Algazar, Hayam E Rashed	
<b>A Prospective Study to Evaluate the Impact of Cancer Directed Treatment on Quality of Life in Head and Neck Cancer Patients</b> .....	61
Sujal Parkar, Abhishek Sharma, Mihir Shah	
<b>“CUIDARAS”: A Nominal and Personalized Health Care Model. Effectiveness of a Massive Screening for Colorectal Cancer Detection at Community level</b> .....	72
Gustavo H. Marin, Hector Trebuca, Carlos Prego, Luis Mosquera, Gustavo Zanelli, Daniela Pena, Gustavo Sanchez, Marcela Mayet, Julieta Spina, Andrea Lalleé, Florencia Scigliano, Adrian Fernandez	

## Case Reports

<b>Pseudotumor of the Infratemporal Fossa Complicated with Orbital Apex Syndromes</b> .....	78
Nik Mohd Syahrul Hafizzi Awang, Rosli Mohd Noor, Rosdi Ramli, Baharudin Abdullah	
<b>A Rare Occurrence: Triple ‘True’ Metachronous Endometrial, Nasal Cavity and Recto-Sigmoid Cancer</b> .....	82
Aashita, Vikas Yadav, Rajiv Sharma, Pragyat Thakur, Hemendra Mishra, Sanchit Jain	
<b>Uterine Perivascular Epithelioid Cell Tumor (PEComa) in A 56-year-Old Woman</b> .....	86
Ala Aljehani, Ahmed Abu-Zaid, Mohamed Ismail Albadawi, Osama Alomar, Abdulmohsen Alkushi	
<b>Intracranial Meningiomas Developed after Traditional Scalp Thermal Cautery Treatment in Childhood: Clinical Reports and Gene Expression Analysis</b> .....	90
Ashwag Alqurashi, Saleh Baeesa, Maher Kurdi, Deema Hussein, Hans-Juergen Schulten	

## Conference Highlights/Scientific Contributions

• <b>News Notes</b> .....	107
• <b>Advertisements</b> .....	110
• <b>Scientific events in the GCC and the Arab World for 2022</b> .....	111

---



## Case Report

# Intracranial Meningiomas Developed after Traditional Scalp Thermal Cautery Treatment in Childhood: Clinical Reports and Gene Expression Analysis

Ashwag Alqurashi<sup>1</sup>, Saleh Baeesa<sup>1</sup>, Maher Kurdi<sup>2</sup>, Deema Hussein<sup>3</sup>, Hans–Juergen Schulten<sup>4</sup>

<sup>1</sup>Division of Neurosurgery, Faculty of Medicine, King Abdulaziz University, Jeddah, Saudi Arabia.

<sup>2</sup>Department of Pathology, Faculty of Medicine, King Abdulaziz University, Jeddah, Saudi Arabia.

<sup>3</sup>King Fahd Medical Research Center, Department of Medical Laboratory Technology, Faculty of Applied Medical Sciences, King Abdulaziz University, Jeddah, Saudi Arabia.

<sup>4</sup>Center of Excellence in Genomic Medicine Research, Department of Medical Laboratory Technology, Faculty of Applied Medical Sciences, King Abdulaziz University, Jeddah, Saudi Arabia.

## Abstract

**Background:** Human skin cautery, a traditional thermal therapy, is traced back to Hippocrates beyond the 5th century. Those ancient healers used this method to control bleeding and infection and remove cancerous tumors. Such traditional procedure is still in practice in several regions of Asia and Africa to treat certain conditions. There is a lack of reports in the literature regarding the long-term complication and the possible tumorigenesis following traditional treatment with thermal cauterization. Here, we report two patients with intracranial meningiomas and investigate the gene expression profile for a patient.

**Cases presentations:** We report two adult patients who presented with a headache and hemiparesis over six months. Brain magnetic resonance imaging (MRI) scans of both patients revealed intracranial meningiomas. During preoperative preparation of the patients, cautery marks

were noticed over the scalp region above the intracranial tumors site, which was performed during childhood. The patients underwent uneventful resection of meningiomas with no local recurrence over a 5-year follow up. In addition, we performed a biofunctional genetic microarray expression analysis on the affected meningioma.

**Conclusion:** There is a lack of evidence–based scientific reports in the literature regarding the long-term complications and tumorigenesis following aggressive treatment with thermal cauterization. Herein, we report the first possible association between previous scalp traditional cautery and the development meningioma in two patients and discuss a proposed causal relationship. However, further advanced studies and research should be done to support, or reject, our hypothesis.

**Keywords:** Traditional medicine. Cautery. Meningioma. Pathogenesis. Gene expression.

## Introduction

Traditional cautery (also known in Arabic as Wasam or Kaiy) remains one of the most ancient forms of therapy that is still currently in practice by healers for treatment, prevention of disease, and or upholding of good health in many developing countries across Asia and Africa<sup>(8,9)</sup>. The ancient Egyptians used cautery to stop bleeding, treat infection and cancer. It was reintroduced in the 10th century by Abu Al–Qasim Al–Zahrawi, an Andalusian physician, as the treatment method using a unique tool called cauters to stop bleeding of arteries. The cauterization technique is performed using a rod metal, the cauter, pointed at one end or often bent at the top into a crescent shape (Figure 1).

The indication for cauterization by the traditional healers included stroke, sciatica, gastroenteritis in children, pneumonia, and mental or psychological problems. The location of the area in the body and the number of cauteries depend on the patient's complaints.

Some early complications from cauterization are occasionally observed, including deep skin burns, cautery

**Corresponding Author:** Saleh Baeesa, MD, FRCSC, FAANS, Professor and Consultant, Division of Neurosurgery, King Abdulaziz University Hospital, Jeddah, Kingdom of Saudi Arabia, Tel:011–966–2–6408207, Fax:011–966–2–6408469, Email: sbaeesa@kau.edu.sa  
ORCID: 0000–0002–3053–7912



**Figure 1. Cautery metal used as a traditional treatment.**



**Figure 2: A midline scalp cauterization marks over the coronal suture region.**

wound infection, delayed wound healing, amputation, tetanus, multiple abscesses, and septic shock. The association between the scalp's thermal cauterization and developing brain tumors has not been described in the literature.

We present the first two cases of parasagittal meningiomas that coincidentally occurred in two patients after traditional scalp cauterization during childhood and discuss possible association. In addition, we show analysis comparing the gene expression profile of affected meningioma with 22 meningioma cases known not to be affected by scalp cauterization.

## Case presentations

### Case report 1

A 57-year-old Saudi Arabian female presented to our institution with a long-standing headache that became

more persistent in the last six months before clinical intervention. There was no neurological deficit. During the patient's evaluation, old cauterization marks were noticed over the scalp (Figure 2). One of the cauterization marks was over the mastoid bone on each side, one was in the occipital area, and the largest one was over the coronal suture on the midline. The patient reported that the procedure was performed at around 7 years of age for gastroenteritis.

Brain magnetic resonance imaging (MRI) scan showed a right frontal parasagittal 35 mm x 43 mm strongly enhanced tumor that was highly suggested for a meningioma (Figure 3). A tumor was located immediately under the cauterization mark.

The patient underwent total microsurgical resection of the tumor and surrounding cuff of dura; the tumor did not involve the sagittal sinus. There were severe adhesions at the scalp layers and the dura around the cauterization during

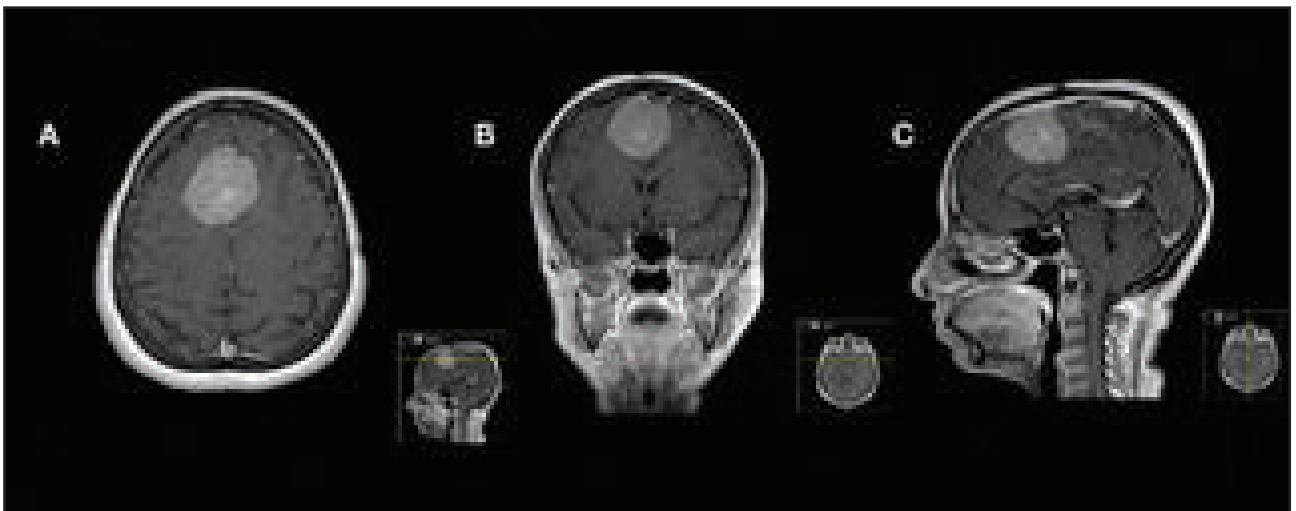


**Figure 3: An axial, coronal, and sagittal brain MRI scan shows contrast-enhanced right frontal parasagittal meningioma.**

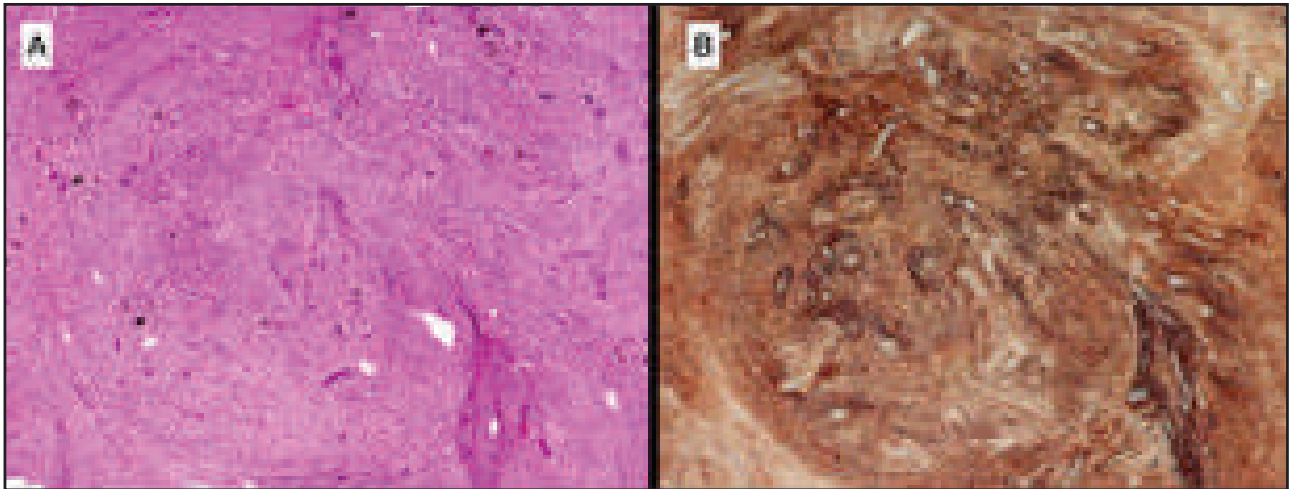


Figure 4: A: H&E histological sections (x10) show WHO grade I meningioma, transitional and psammomatous types. B: The cells demonstrated strong immunoreactivity for EMA.

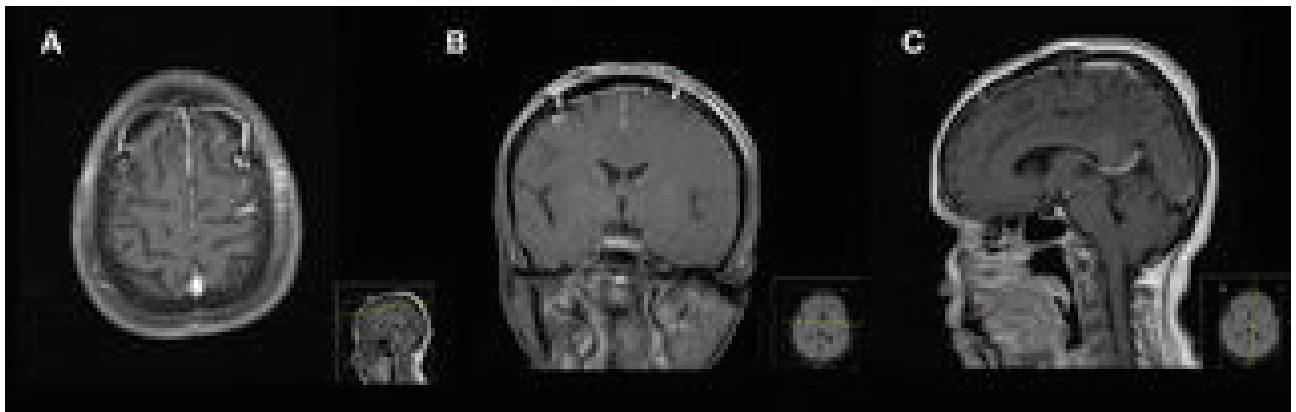


Figure 5: Postoperative axial, coronal, and sagittal enhanced brain MRI scan follow up at five years showing no tumor recurrence.

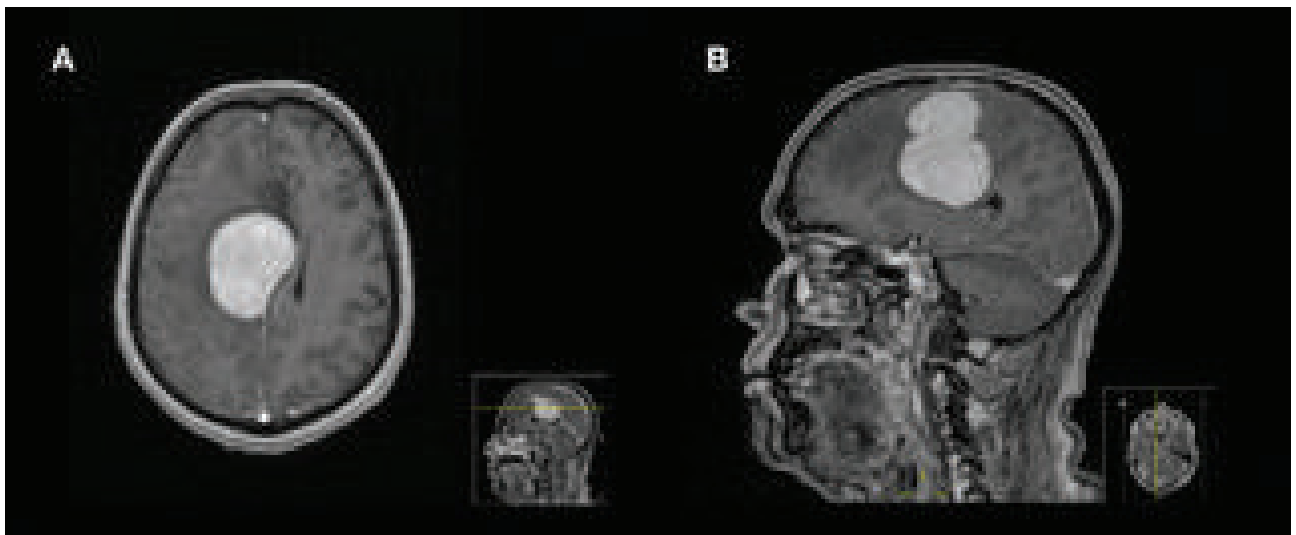


Figure 6: Multiple midline scalp cautery marks over the scalp region.

a frontal craniotomy, but no skull defect was noted. Histopathological examination of the tissue revealed a WHO grade 1 meningioma, mixed psammomatous with transitional types (Figure 2c). The tumor cells were strongly positive for Epithelial membrane antigen immunohistochemical staining (Figure 4). The patient had an uneventful recovery, and she remained with no evidence of local recurrence on a 5-year follow-up MRI scan (Figure 5).

### Case report 2

A 66-year-old Saudi Arabian male presented to our institution with a ten-month history of headaches and recent progressive left leg weakness. During the patient's examination, which revealed left leg moderate paraparesis, three midline cautery marks were noticed over the scalp region and posterior to the coronal suture (Figure 6). The patient reported that the cautery was performed around 10 years of age for febrile illness. Brain MRI scan showed a 40 mm x 48 mm strongly enhanced tumor with marked mass effect and surrounding edema in the right frontal area that suggested a meningioma (Figure 7).



**Figure 7:** An axial and sagittal brain MRI scan demonstrating a contrast-enhanced large right falx meningioma with marked mass effect and vasogenic edema.

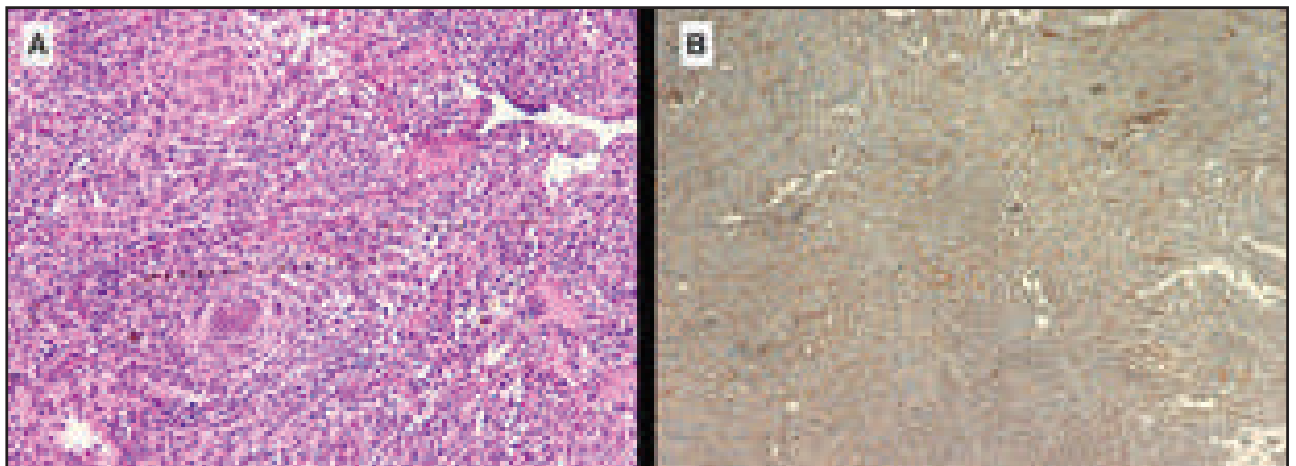


**Figure 8:** A: H&E histological sections (x10) show WHO grade II atypical meningioma. B: there is a focal invasion to the brain parenchyma seen with GFAP stain.

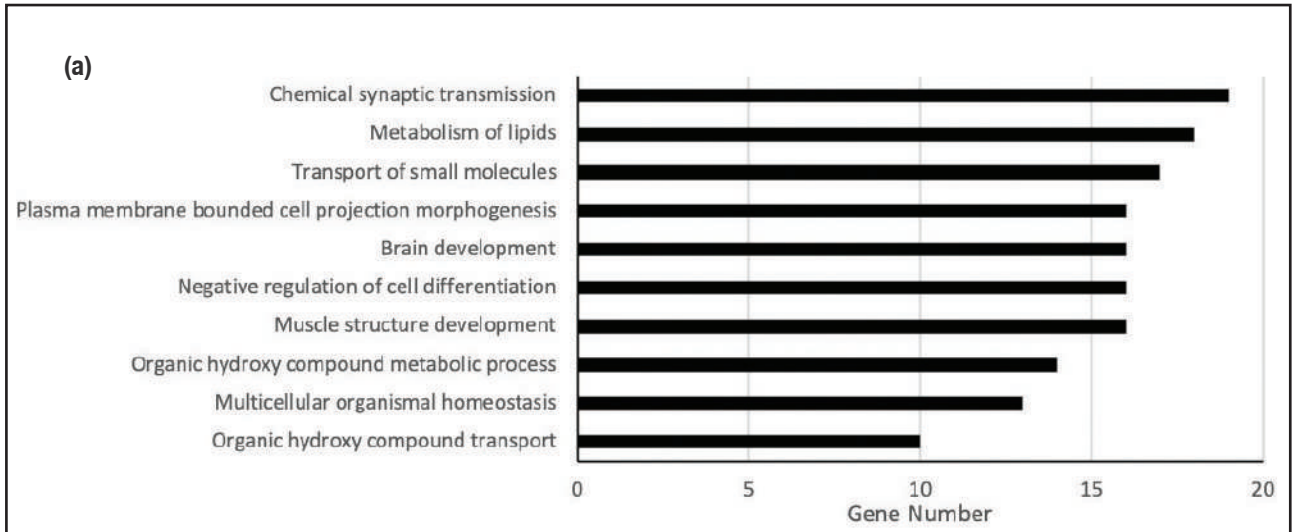


**Figure 9:** Postoperative axial, coronal, and sagittal enhanced brain MRI scan follow up at five years showing no tumor recurrence.

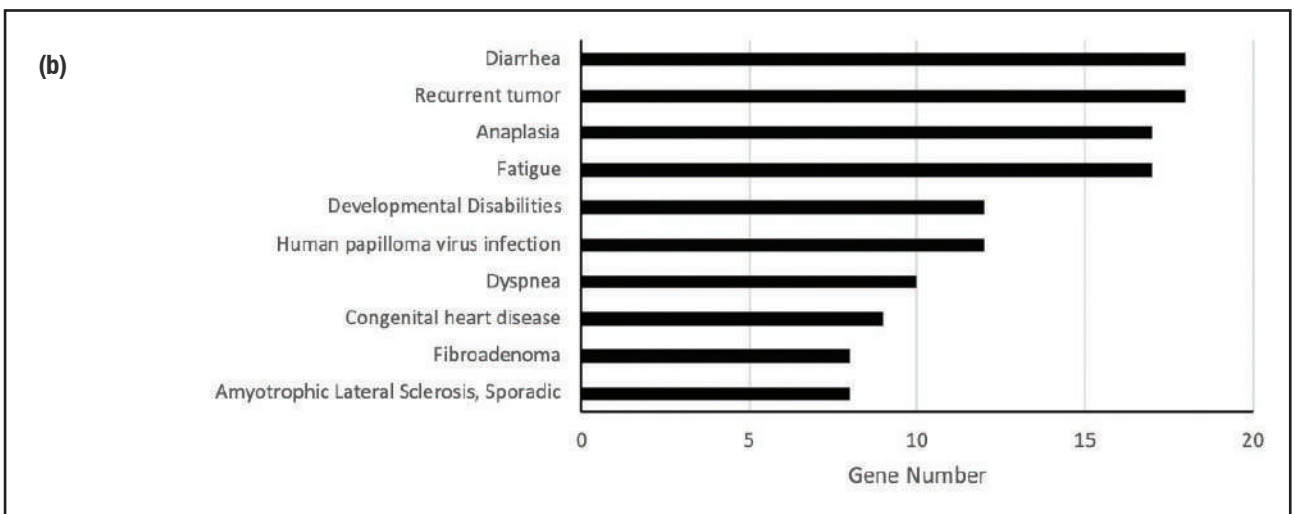
Total microsurgical resection of the tumor with its surrounding falx attachment has been performed through a right frontal craniotomy; the sagittal sinus was not involved. During exposure, marked adhesions were observed during scalp and dura dissection, but no bone abnormality was noted.

Histopathological examination of the tissue revealed a WHO grade II atypical meningioma (Figure 8). The glial fibrillary acidic protein immunohistochemical staining highlighted the focal invasion to the brain parenchyma (Figure 3d).

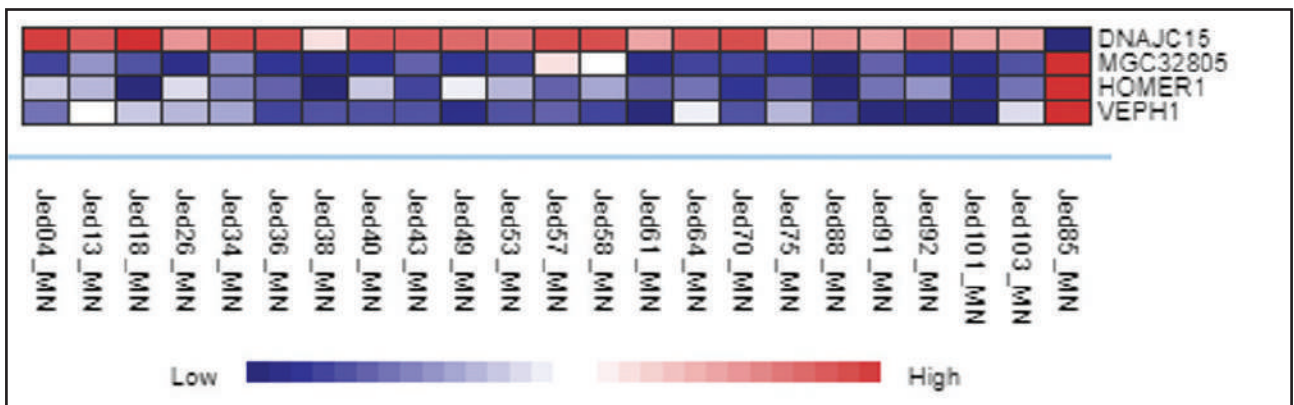
**Figure 10: The differential gene expression profile for affected compared with 22 meningiomas with no head cauterization history.**



**a) The top ten deregulated enriched pathways for 323 differentially expressed genes.**



**b) The top ten pathways identified following enrichment analysis in gene-disease associations database (DisGeNET).**

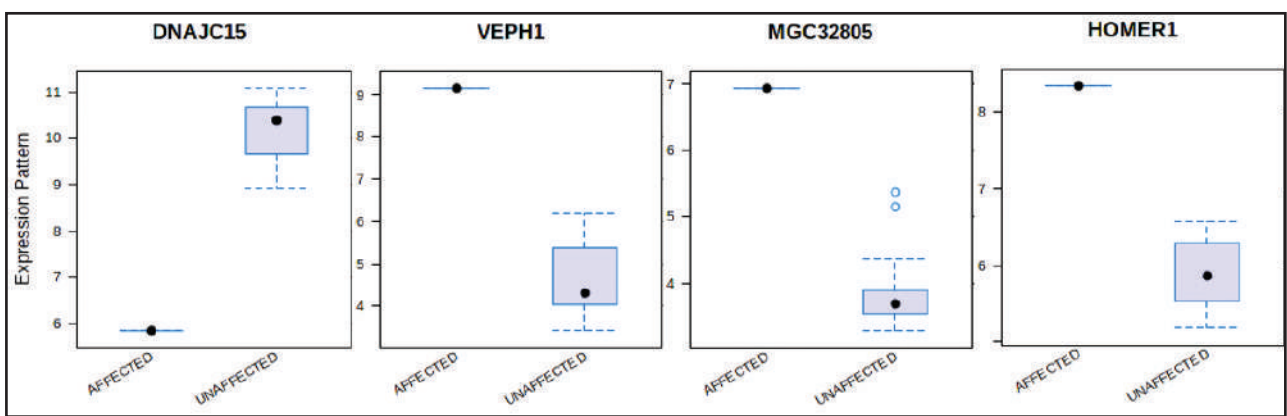


**c) A heat map for the most significantly deregulated genes in tissues retrieved.**

The patient had a remarkable recovery of his left leg monoparesis within a few weeks following surgery and remained with no evidence of meningioma recurrence for a 5-year follow up with an MRI scan (Figure 9).

### Microarray expression analysis

In order to identify possible intrinsic genomic features that might be unique to tumor tissues derived from the affected meningioma, the microarray expression values



d) Box blots showing the comparative levels of expression for DNAJC15, VEPH1, MGC32805, and HOMER1.

ID	logFC	AveExpr	P.Value	adj.P.Val
DNAJC15	-4.3421	9.9961	1.64E-08	0.000273
VEPH1	4.5856	4.762	8.28E-06	0.034569
MGC32805	3.0955	3.9693	2.61E-06	0.021747
HOMER1	2.4677	5.9796	5.59E-06	0.031107

**Table 1. The most significantly deregulated genes in tissues were retrieved from affected compared with 22 meningiomas with no history of scalp cautery.**

of meningioma samples were reanalyzed for differentially expression analysis between meningioma samples collected from our cohort (GEO submissions GSE100534 and GSE77259<sup>(19)</sup>). The 22 control meningiomas are known to have a history free from skin cautery. The gene expression values were analyzed using the NetworkAnalyst 3.0 platform. The variance filter was set to a percentile rank of 15, and the relative abundance tab was set to 5. A  $p$ -value  $\leq$  of 0.05 was used, and no further normalization was applied since the data had been normalized initially. A Limma statistical test was then used to compare the differential gene expression values between affected and 22 control meningioma cases (Unaffected). Low relative abundance and low variances genes based on IQR were filtered. Out of 25293 initially included genes, 16692 genes were finally selected for differential analysis. In total, 323 genes were statistically differentially expressed in affected cases than the other meningiomas (Supplementary Table 1). Out of the differentially expressed genes, 231 genes were downregulated, and 92 genes were upregulated. Out of all differentially expressed genes, DNAJC15 (DNAJ heat shock protein family (Hsp40) member C15) was the most significantly downregulated gene, and MGC32805 (uncharacterized LOC153163), HOMER1 (homer scaffold protein 1), and VEPH1 (ventricular zone expressed PH domain containing 1) were the most significantly down-regulated in the unaffected set (Table 1, Figures 10c and 10d). The top enriched pathways for these genes

included Chemical synaptic transmission, Metabolism of lipids, Transport of small molecules, Plasma membrane-bounded cell projection morphogenesis, and Brain development (Figure 10a). The top pathways identified following enrichment analysis in the database of gene-disease associations (DisGeNET) included Diarrhea, Recurrent tumor, Anaplasia, Fatigue, Developmental Disabilities, and Human papillomavirus (HPV) infection (Figure 10b).

## Discussion

Traditional Cautery is still in-practice in several regions of the world<sup>(8,9)</sup>. The exact pathophysiology is not clear. It is believed that the thermal waves are transmitted through the affected areas to control pain, bleeding, and infection and to remove the cancerous skin tumors. It is also thought that it prevents the spreading of the disease to healthy organs, enhances the body's healing energy, and increases new blood cells' production. Traditional practitioners believe that pain relief is achieved by intense heat destruction to the pathogenic substances inside the body, others believe it may act in the same way as acupuncture, stimulating the release of endogenous opioids and other neurotransmitters that prevent the feeling of pain that is a natural physiological body method to avoid the feeling of severe pain<sup>(1)</sup>.

While cautery use for infectious or inflammatory and cancer conditions, traditional practitioners believed that cautery might affect and improve the body's defense mechanisms and immunity. However, in an experimental animal study, total white blood cells and differential count were significantly altered after thermal injury, particularly depression in the peripheral polymorphonuclear leukocytes phagocytic capacity<sup>(8)</sup>. One study that looked at patients with breast cancer, who received traditional cautery, found that they have higher and early loco-regional spread. The authors postulated that it might be due to increased local temperature and edema following

<b>Symbols</b>	<b>Name</b>	<b>logFC</b>	<b>AveExpr</b>	<b>P.Value</b>
DNAJC15	DnaJ heat shock protein family (Hsp40) member C15	-4.3421	9.9961	1.64E-08
EBF1	EBF transcription factor 1	-2.7807	9.6223	0.00073714
ATP1B1	ATPase Na <sup>+</sup> /K <sup>+</sup> transporting subunit beta 1	-2.6948	10.209	0.0032402
LDOC1	LDOC1 regulator of NFKB signaling	-2.63	8.3594	0.040093
ELOVL2	ELOVL fatty acid elongase 2	-2.4989	8.1742	0.039415
SLC15A2	solute carrier family 15 member 2	-2.4334	8.0314	0.012527
FCGBP	Fc fragment of IgG binding protein	-2.4288	9.3786	0.043265
ENPP2	ectonucleotide pyrophosphatase/phosphodiesterase 2	-2.3231	9.0569	0.044906
MEG3	maternally expressed 3	-2.2524	7.7593	0.023816
AKR1C2	aldo-keto reductase family 1 member C2	-2.1062	7.5005	0.018903
ID3	"inhibitor of DNA binding 3, HLH protein"	-2.0487	9.7469	0.0013311
SIX2	SIX homeobox 2	-1.9708	10.256	0.032883
ID1	"inhibitor of DNA binding 1, HLH protein"	-1.9384	10.772	0.017367
RNFT2	"ring finger protein, transmembrane 2"	-1.8908	7.2986	0.048024
SPATA18	spermatogenesis associated 18	-1.6614	7.4058	0.038404
ATP10A	ATPase phospholipid transporting 10A (putative)	-1.6541	6.404	0.010837
RNU6-446P	"RNA, U6 small nuclear 446, pseudogene"	-1.6306	4.9605	0.04599
SLC26A6	solute carrier family 26 member 6	-1.5919	8.5663	0.0091998
MT1E	metallothionein 1E	-1.5898	8.0804	0.042381
MT1L	"metallothionein 1L, pseudogene"	-1.5068	8.7754	0.029016
MT1P3	metallothionein 1 pseudogene 3	-1.4778	7.1479	0.044703
CA5A	carbonic anhydrase 5A	-1.4464	4.5469	0.022626
DCBLD2	"discoidin, CUB and LCCL domain containing 2"	-1.4452	9.2135	0.013429
ADAM20P1	ADAM metalloproteinase domain 20 pseudogene 1	-1.4271	3.7094	0.017476
ARSJ	arylsulfatase family member J	-1.4102	5.6312	0.041479
STK36	serine/threonine kinase 36	-1.4087	7.7378	0.00085567
MAP3K6	mitogen-activated protein kinase kinase kinase 6	-1.3987	8.3019	0.0099983
FOXC2	forkhead box C2	-1.395	9.8263	0.0087172
CHPF	chondroitin polymerizing factor	-1.395	9.2001	0.036643
BTN3A3	butyrophilin subfamily 3 member A3	-1.3837	7.5926	0.044244
CNNM1	cyclin and CBS domain divalent metal cation transport mediator 1	-1.356	5.7308	0.040636
FBXW10	F-box and WD repeat domain containing 10	-1.3318	4.2078	0.034062
ABCA2	ATP binding cassette subfamily A member 2	-1.3165	8.0562	0.015506
LOC728715	ovostatin homolog 2	-1.307	4.4142	0.041845
TLE1	"TLE family member 1, transcriptional corepressor"	-1.3032	7.5616	0.049241
APLP1	amyloid beta precursor like protein 1	-1.2842	7.7717	0.046231
FIGN	"fidgetin, microtubule severing factor"	-1.283	8.6988	0.030461
PLGLB2	plasminogen like B2	-1.2815	4.7336	0.0070854

RNU2–52P	“RNA, U2 small nuclear 52, pseudogene”	–1.2794	4.5375	0.032089
RNU6–824P	“RNA, U6 small nuclear 824, pseudogene”	–1.2707	4.2811	0.016101
LRRTM2	leucine rich repeat transmembrane neuronal 2	–1.2622	5.3634	0.0098794
IKZF2	IKAROS family zinc finger 2	–1.2387	7.0111	0.00030039
GPR85	G protein–coupled receptor 85	–1.2314	4.6414	0.022618
PDZD9	PDZ domain containing 9	–1.2234	3.7499	0.0329
CPVL	carboxypeptidase vitellogenic like	–1.2131	7.3964	0.040611
RNU6–14P	“RNA, U6 small nuclear 14, pseudogene”	–1.2068	3.5198	0.0058796
PGA3	pepsinogen A3	–1.1798	5.6636	0.045812
RSRP1	arginine and serine rich protein 1	–1.1648	7.541	0.015866
MEIS1	Meis homeobox 1	–1.1588	4.9392	0.023251
TTLL3	tubulin tyrosine ligase like 3	–1.1565	8.5721	0.024597
ZNF142	zinc finger protein 142	–1.1493	8.0218	0.0014867
RNA5SP136	“RNA, 5S ribosomal pseudogene 136”	–1.1481	3.508	0.035195
CENPI	centromere protein I	–1.1434	5.4269	0.043629
STPG1	sperm tail PG–rich repeat containing 1	–1.1433	7.3093	0.027887
LDLRAP1	low density lipoprotein receptor adaptor protein 1	–1.1417	8.1383	0.040389
TNFRSF14	TNF receptor superfamily member 14	–1.1409	7.8784	0.026224
LANCL1	LanC like 1	–1.1396	9.4499	0.025535
ZNF100	zinc finger protein 100	–1.1319	7.175	0.041158
ASIC1	acid sensing ion channel subunit 1	–1.1312	6.2703	0.047931
GMPPA	GDP–mannose pyrophosphorylase A	–1.124	8.371	0.021011
KLF7	Kruppel like factor 7	–1.1226	10.157	0.032302
RNA5SP124	“RNA, 5S ribosomal pseudogene 124”	–1.1204	4.5331	0.036207
CUZD1	CUB and zona pellucida like domains 1	–1.1135	4.8514	0.03819
RNU6–421P	“RNA, U6 small nuclear 421, pseudogene”	–1.1062	4.5526	0.016838
RN7SL325P	“RNA, 7SL, cytoplasmic 325, pseudogene”	–1.1012	3.8732	0.033256
NUMBL	NUMB like endocytic adaptor protein	–1.0987	8.6261	0.010822
DPYSL4	dihydropyrimidinase like 4	–1.0969	7.1768	0.033409
RGS9	regulator of G protein signaling 9	–1.0883	5.5502	0.0044633
RNU6–1045P	“RNA, U6 small nuclear 1045, pseudogene”	–1.0857	4.0908	0.042262
RN7SKP297	RN7SK pseudogene 297	–1.0844	4.3346	0.037269
DPRX	divergent–paired related homeobox	–1.0755	5.4087	0.047065
CDC42	cell division cycle 42	–1.0742	7.148	0.0076148
PPM1K	“protein phosphatase, Mg <sup>2+</sup> /Mn <sup>2+</sup> dependent 1K”	–1.0714	6.0779	0.029599
RN7SL446P	“RNA, 7SL, cytoplasmic 446, pseudogene”	–1.0638	3.6413	0.029044
TPRX1	tetrapeptide repeat homeobox 1	–1.0612	5.2962	0.049495
TTLL4	tubulin tyrosine ligase like 4	–1.048	7.8535	0.035872
FDXR	ferredoxin reductase	–1.0463	6.8429	0.028833
IDI2	isopentenyl–diphosphate delta isomerase 2	–1.0367	4.065	0.028051

LOC153684	uncharacterized LOC153684	-1.0358	7.343	0.041762
RNA5SP378	"RNA, 5S ribosomal pseudogene 378"	-1.0337	5.2027	0.0383
SRRM1	serine and arginine repetitive matrix 1	-1.0308	9.411	0.013078
DGCR6	DiGeorge syndrome critical region gene 6	-1.0253	7.0306	0.01368
RNU2-40P	"RNA, U2 small nuclear 40, pseudogene"	-1.0143	4.0104	0.039847
RNA5SP152	"RNA, 5S ribosomal pseudogene 152"	-1.0046	4.3282	0.04956
B3GAT1	"beta-1,3-glucuronyltransferase 1"	-0.99341	5.5782	0.041222
LHX5	LIM homeobox 5	-0.99308	5.5201	0.028475
COL5A1	collagen type V alpha 1 chain	-0.99161	7.2063	0.027003
SSXP1	SSX family pseudogene 1	-0.99159	4.4167	0.02717
RNU1-49P	"RNA, U1 small nuclear 49, pseudogene"	-0.99116	4.3674	0.02469
RN7SL782P	"RNA, 7SL, cytoplasmic 782, pseudogene"	-0.98485	5.8188	0.03714
RN7SKP228	RN7SK pseudogene 228	-0.97895	4.8734	0.046659
SPATA20	spermatogenesis associated 20	-0.97881	9.2174	0.04944
RNA5SP496	"RNA, 5S ribosomal pseudogene 496"	-0.96558	3.6526	0.048428
ANKRD55	ankyrin repeat domain 55	-0.96335	4.3281	0.044285
UCN2	urocortin 2	-0.96225	5.8901	0.0089121
LRIT1	"leucine rich repeat, Ig-like and transmembrane domains 1"	-0.96183	5.086	0.038031
DHDDS	dehydrodolichyl diphosphate synthase subunit	-0.96083	9.0023	0.046827
RNU1-84P	"RNA, U1 small nuclear 84, pseudogene"	-0.95991	3.8127	0.0357
RNU6-625P	"RNA, U6 small nuclear 625, pseudogene"	-0.94278	3.4331	0.013301
NPTX2	neuronal pentraxin 2	-0.93952	5.9306	0.013487
RPE	ribulose-5-phosphate-3-epimerase	-0.93849	7.84	0.027454
RDM1	RAD52 motif containing 1	-0.93744	4.3275	0.02811
COPS7B	COP9 signalosome subunit 7B	-0.93412	7.9422	0.0074281
C5orf52	chromosome 5 open reading frame 52	-0.92896	3.9616	0.018685
SOX5	SRY-box transcription factor 5	-0.92713	5.3381	0.041409
RNU6-1158P	"RNA, U6 small nuclear 1158, pseudogene"	-0.92456	6.3442	0.0032012
OR4D11	olfactory receptor family 4 subfamily D member 11	-0.92278	4.189	0.039036
STAR	steroidogenic acute regulatory protein	-0.91959	5.0395	0.034743
RNA5SP213	"RNA, 5S ribosomal pseudogene 213"	-0.91932	3.2369	0.032164
FAM122C	family with sequence similarity 122C	-0.91833	7.8213	0.034795
MARCKSL1	MARCKS like 1	-0.91801	10.117	0.033014
REG3G	regenerating family member 3 gamma	-0.91274	3.3933	0.008073
RARA	retinoic acid receptor alpha	-0.91052	7.7266	0.01959
BCS1L	"BCS1 homolog, ubiquinol-cytochrome c reductase complex chaperone"	-0.91018	7.6962	0.024376
GLRB	glycine receptor beta	-0.90964	3.6784	0.035075
GAST	gastrin	-0.9091	5.6892	0.017135
RNA5SP169	"RNA, 5S ribosomal pseudogene 169"	-0.90626	4.0988	0.042253

RN7SL709P	“RNA, 7SL, cytoplasmic 709, pseudogene”	-0.90396	5.1274	0.034145
LINC00308	long intergenic non-protein coding RNA 308	-0.90375	3.4793	0.034456
TRPC5	transient receptor potential cation channel subfamily C member 5	-0.9025	4.3545	0.03407
SPAG16	sperm associated antigen 16	-0.90223	6.9235	0.048588
SNORA71C	“small nucleolar RNA, H/ACA box 71C”	-0.90199	8.1497	0.024591
PMP22	peripheral myelin protein 22	-0.90141	11.83	0.033576
POU5F1B	POU class 5 homeobox 1B	-0.90068	5.6514	0.045868
SETBP1	SET binding protein 1	-0.89547	8.8322	0.026368
RNU6-64P	“RNA, U6 small nuclear 64, pseudogene”	-0.8924	4.3835	0.044514
MTERF4	mitochondrial transcription termination factor 4	-0.89206	6.4639	0.013573
OR2T35	olfactory receptor family 2 subfamily T member 35	-0.8914	4.537	0.02115
C15orf61	chromosome 15 open reading frame 61	-0.88868	6.4299	0.029277
AHDC1	AT-hook DNA binding motif containing 1	-0.88831	7.4483	0.025793
OR8B1P	olfactory receptor family 8 subfamily B member 1 pseudogene	-0.88391	3.5929	0.037582
ELOVL2-AS1	ELOVL2 antisense RNA 1	-0.88299	3.7842	0.029765
DAND5	DAN domain BMP antagonist family member 5	-0.88104	5.1395	0.024554
CDR2L	cerebellar degeneration related protein 2 like	-0.87384	6.5948	0.040018
UPB1	beta-ureidopropionase 1	-0.87035	4.9894	0.013516
KRT35	keratin 35	-0.86678	5.0509	0.01732
CCDC84	coiled-coil domain containing 84	-0.86646	8.4796	0.032459
EME1	essential meiotic structure-specific endonuclease 1	-0.86454	5.1888	0.023234
POU6F1	POU class 6 homeobox 1	-0.86023	7.1111	0.03897
TMEM163	transmembrane protein 163	-0.85614	5.1079	0.045744
GLT6D1	glycosyltransferase 6 domain containing 1	-0.85551	3.848	0.02103
C20orf141	chromosome 20 open reading frame 141	-0.84714	5.5603	0.018917
RN7SL15P	“RNA, 7SL, cytoplasmic 15, pseudogene”	-0.84613	5.6854	0.026572
SNORA70D	“small nucleolar RNA, H/ACA box 70D”	-0.8351	5.2037	0.023512
HSF4	heat shock transcription factor 4	-0.83417	7.7863	0.039038
RNU6-388P	“RNA, U6 small nuclear 388, pseudogene”	-0.83339	4.7318	0.046158
MICALCL	MICAL C-terminal like	-0.8297	5.4655	0.036985
MIR152	microRNA 152	-0.82527	5.8305	0.040982
MAGEE2	MAGE family member E2	-0.8231	4.9029	0.043855
CD79A	CD79a molecule	-0.81875	5.8085	0.048428
BDNF	brain derived neurotrophic factor	-0.81767	4.0456	0.028524
DDX4	DEAD-box helicase 4	-0.81683	3.6195	0.018869
C10orf55	chromosome 10 open reading frame 55 (putative)	-0.81454	3.9084	0.027764
SLC30A8	solute carrier family 30 member 8	-0.81114	4.4904	0.026609
CNGA2	cyclic nucleotide gated channel subunit alpha 2	-0.80653	4.6069	0.031856
RN7SL833P	“RNA, 7SL, cytoplasmic 833, pseudogene”	-0.80168	5.788	0.016773

TACR1	tachykinin receptor 1	-0.80165	4.5619	0.025526
RN7SL251P	"RNA, 7SL, cytoplasmic 251, pseudogene"	-0.79185	3.9961	0.03462
DIS3L2	DIS3 like 3'-5' exoribonuclease 2	-0.78923	7.8589	0.032507
OSBPL7	oxysterol binding protein like 7	-0.78811	7.3784	0.028944
RN7SL466P	"RNA, 7SL, cytoplasmic 466, pseudogene"	-0.78734	3.2534	0.036229
S100A7L2	S100 calcium binding protein A7 like 2	-0.78706	3.2331	0.042562
VSTM2L	V-set and transmembrane domain containing 2 like	-0.78515	6.9977	0.040798
HAUS7	HAUS augmin like complex subunit 7	-0.78457	7.0901	0.029202
SLC37A1	solute carrier family 37 member 1	-0.78382	6.3682	0.045727
RN7SKP122	RN7SK pseudogene 122	-0.78331	4.0876	0.024718
CYP4A11	cytochrome P450 family 4 subfamily A member 11	-0.78305	4.6669	0.029437
NXNL2	nucleoredoxin like 2	-0.78213	6.1347	0.045529
RN7SKP237	RN7SK pseudogene 237	-0.77646	5.6079	0.047654
TNFRSF25	TNF receptor superfamily member 25	-0.77455	7.6749	0.039538
ZSCAN20	zinc finger and SCAN domain containing 20	-0.77275	6.16	0.016959
RNU6-365P	"RNA, U6 small nuclear 365, pseudogene"	-0.7667	3.3795	0.024194
PAQR4	progesterin and adipoQ receptor family member 4	-0.76517	7.4165	0.0093763
OR1A1	olfactory receptor family 1 subfamily A member 1 (gene/ pseudogene)	-0.76273	4.3427	0.017284
TCF21	transcription factor 21	-0.76266	4.7798	0.025591
RNA5SP479	"RNA, 5S ribosomal pseudogene 479"	-0.75834	3.9815	0.017569
PON2	paraoxonase 2	-0.75488	9.8377	0.049604
RNA5SP175	"RNA, 5S ribosomal pseudogene 175"	-0.75391	5.2128	0.026005
AQP5	aquaporin 5	-0.74842	6.2301	0.026323
SNAI1P1	snail family zinc finger 1 pseudogene 1	-0.74343	4.8432	0.027259
MAGEB5	MAGE family member B5	-0.74215	3.5925	0.017285
HMGNP2P1	high mobility group nucleosomal binding domain 2 pseudogene 21	-0.73971	5.4966	0.039701
RN7SL559P	"RNA, 7SL, cytoplasmic 559, pseudogene"	-0.73809	5.589	0.026467
RAET1E-AS1	RAET1E antisense RNA 1	-0.73679	6.2649	0.045033
LOC400499	putative uncharacterized protein LOC400499	-0.73624	5.0322	0.047113
CHRD2	chordin like 2	-0.73535	5.7639	0.039059
SLC26A9	solute carrier family 26 member 9	-0.73395	4.9596	0.034272
OR2W6P	olfactory receptor family 2 subfamily W member 6 pseudogene	-0.72536	3.9971	0.025786
LRRTM1	leucine rich repeat transmembrane neuronal 1	-0.72204	4.943	0.048207
PLAC4	placenta enriched 4	-0.71614	4.3473	0.040577
SPACA4	sperm acrosome associated 4	-0.71591	4.0994	0.031634
C16orf95	chromosome 16 open reading frame 95	-0.71389	6.1771	0.048127
PHACTR3	phosphatase and actin regulator 3	-0.71313	5.8006	0.034634
RNU6-131P	"RNA, U6 small nuclear 131, pseudogene"	-0.71243	3.5172	0.044922

LYPLA2	lysophospholipase 2	-0.7122	7.9272	0.03245
KCNAB3	potassium voltage-gated channel subfamily A regulatory beta subunit 3	-0.7098	4.9842	0.042354
KRTAP12-3	keratin associated protein 12-3	-0.7079	6.0302	0.046919
RNU6-1250P	"RNA, U6 small nuclear 1250, pseudogene"	-0.7077	3.6442	0.041555
AVP	arginine vasopressin	-0.70745	6.2407	0.029143
CIB4	calcium and integrin binding family member 4	-0.70721	4.2521	0.030974
RN7SL420P	"RNA, 7SL, cytoplasmic 420, pseudogene"	-0.70254	5.69	0.018834
RAB40B	"RAB40B, member RAS oncogene family"	-0.69716	7.7348	0.034548
ZDHHC8P1	ZDHHC8 pseudogene 1	-0.69701	6.846	0.04162
FAM163A	family with sequence similarity 163 member A	-0.69554	4.6208	0.039036
MIR412	microRNA 412	-0.69486	3.988	0.047721
PLEKHH3	"pleckstrin homology, MyTH4 and FERM domain containing H3"	-0.69425	7.2804	0.037624
RNA5SP430	"RNA, 5S ribosomal pseudogene 430"	-0.69302	4.9379	0.042824
CNOT3	CCR4-NOT transcription complex subunit 3	-0.6922	7.793	0.044583
BAIAP3	BAI1 associated protein 3	-0.67645	6.0327	0.044034
CPN2	carboxypeptidase N subunit 2	-0.67355	5.7849	0.045782
TBX22	T-box transcription factor 22	-0.67277	3.6596	0.0372
RSAD1	radical S-adenosyl methionine domain containing 1	-0.67196	7.3504	0.027963
OR4A21P	olfactory receptor family 4 subfamily A member 21 pseudogene	-0.67135	4.1315	0.048561
DHRS7C	dehydrogenase/reductase 7C	-0.66716	5.0465	0.040788
TBATA	"thymus, brain and testes associated"	-0.65817	4.8066	0.046822
TTY6	"testis-specific transcript, Y-linked 6"	-0.64453	4.3603	0.030735
RNA5-8SP5	"RNA, 5.8S ribosomal pseudogene 5"	-0.6429	3.4094	0.043592
SAPCD2	suppressor APC domain containing 2	-0.64232	6.3302	0.048975
SYNGR4	synaptogyrin 4	-0.63454	6.1083	0.044062
SRCIN1	SRC kinase signaling inhibitor 1	-0.63276	6.0048	0.035438
SNORA35	"small nucleolar RNA, H/ACA box 35"	-0.62362	5.2343	0.045558
GDF3	growth differentiation factor 3	-0.6216	3.6241	0.045939
RN7SL499P	"RNA, 7SL, cytoplasmic 499, pseudogene"	-0.61401	3.2806	0.036946
ITLN2	intelectin 2	-0.61192	4.2414	0.043032
PSTPIP1	proline-serine-threonine phosphatase interacting protein 1	-0.608	6.2159	0.044808
ZP1	zona pellucida glycoprotein 1	-0.60673	5.2347	0.045029
FGB	fibrinogen beta chain	-0.60256	3.9612	0.04932
HIGD2B	HIG1 hypoxia inducible domain family member 2B	-0.59291	4.6673	0.038331
SYCE2	synaptonemal complex central element protein 2	-0.59238	5.0838	0.049937
UNC5A	unc-5 netrin receptor A	-0.57633	6.081	0.042381
CD7	CD7 molecule	-0.56243	8.0148	0.043628
CHRND	cholinergic receptor nicotinic delta subunit	0.62671	5.3661	0.023177

LRRC46	leucine rich repeat containing 46	0.64597	4.673	0.045955
SPTY2D1	SPT2 chromatin protein domain containing 1	0.65573	6.2077	0.032466
RANBP2	RAN binding protein 2	0.65696	8.6995	0.045908
CYSTM1	cysteine rich transmembrane module containing 1	0.65807	8.5685	0.048671
RASL11A	RAS like family 11 member A	0.71408	5.3859	0.046629
RAPGEF2	Rap guanine nucleotide exchange factor 2	0.73571	8.396	0.031323
THUMPD1	THUMP domain containing 1	0.79077	7.9556	0.036532
ARHGEF12	Rho guanine nucleotide exchange factor 12	0.80451	9.802	0.025612
CA7	carbonic anhydrase 7	0.82307	5.2071	0.025546
OSBPL1A	oxysterol binding protein like 1A	0.85229	7.4744	0.017789
ABTB2	ankyrin repeat and BTB domain containing 2	0.86307	6.7485	0.031595
UACA	uveal autoantigen with coiled-coil domains and ankyrin repeats	0.89345	9.0383	0.047426
CYP1B1-AS1	CYP1B1 antisense RNA 1	0.90282	5.1388	0.021826
ABHD2	abhydrolase domain containing 2	0.90584	9.3443	0.04589
RNASEL	ribonuclease L	0.92269	7.0927	0.031024
SRF	serum response factor	0.95017	8.9731	0.0089736
MICU3	mitochondrial calcium uptake family member 3	0.95545	6.7092	0.030141
SIK2	salt inducible kinase 2	0.95932	10.138	0.040549
CREM	cAMP responsive element modulator	0.96789	6.0114	0.018833
SH3BGR	SH3 domain binding glutamate rich protein	0.98395	5.2551	0.026651
LGALS3	galectin 3	1.0308	7.8761	0.046182
STEAP1	STEAP family member 1	1.0407	3.9971	0.029513
TUFT1	tuftelin 1	1.0426	6.937	0.026434
PGAP1	post-GPI attachment to proteins inositol deacylase 1	1.0537	8.1258	0.028378
SLC43A1	solute carrier family 43 member 1	1.0656	8.3571	0.01744
PITPNM3	PITPNM family member 3	1.0664	6.152	0.042262
ZNF10	zinc finger protein 10	1.0696	5.7408	0.020112
ZDBF2	zinc finger DBF-type containing 2	1.0718	6.9779	0.039051
PECR	peroxisomal trans-2-enoyl-CoA reductase	1.0721	7.8329	0.036397
ARG2	arginase 2	1.1029	6.2656	0.0049717
ANKRD28	ankyrin repeat domain 28	1.1206	8.0095	0.0095289
SHANK2	SH3 and multiple ankyrin repeat domains 2	1.1329	5.8088	0.010962
UAP1	UDP-N-acetylglucosamine pyrophosphorylase 1	1.1633	8.1693	0.0073731
RN7SKP35	RN7SK pseudogene 35	1.1656	4.8724	0.046786
ASIP	agouti signaling protein	1.1684	5.7938	0.0286
C3orf36	chromosome 3 putative open reading frame 36	1.1786	5.1289	0.012577
FAM131B	family with sequence similarity 131 member B	1.1872	7.3828	0.045488
RP9P	RP9 pseudogene	1.2078	7.3266	0.0040451
NEMF	nuclear export mediator factor	1.2274	8.763	0.0059647

HSPH1	heat shock protein family H (Hsp110) member 1	1.2535	8.9756	0.037733
PIFO	primary cilia formation	1.2635	5.451	0.042721
DIXDC1	DIX domain containing 1	1.3133	7.9619	0.031455
ITGA10	integrin subunit alpha 10	1.3358	8.0143	0.027424
PRR5L	proline rich 5 like	1.3498	7.501	0.03307
STRIP2	striatin interacting protein 2	1.3617	7.0483	0.015102
GLCE	glucuronic acid epimerase	1.3756	10.113	0.036518
INSRR	insulin receptor related receptor	1.3867	5.6009	0.0039259
PCP4L1	Purkinje cell protein 4 like 1	1.3943	6.7281	0.031565
ARRDC4	arrestin domain containing 4	1.4088	7.7596	0.019454
UBXN10	UBX domain protein 10	1.4394	6.0397	0.020513
CAV1	caveolin 1	1.4544	9.932	0.030626
ABHD3	abhydrolase domain containing 3	1.4559	6.8675	0.042783
WNT2B	Wnt family member 2B	1.4978	6.8189	0.017604
PPP4R4	protein phosphatase 4 regulatory subunit 4	1.4984	4.7415	0.0055205
PTPRE	protein tyrosine phosphatase receptor type E	1.5284	9.1166	0.035015
TFRC	transferrin receptor	1.5416	8.5777	0.039456
PRMT9	protein arginine methyltransferase 9	1.5452	7.7998	0.00037162
DLGAP1	DLG associated protein 1	1.587	6.6443	0.047981
SSPN	sarcospan	1.5991	8.9782	0.031151
GAL	galanin and GMAP prepropeptide	1.6081	6.7864	0.030639
SLC25A19	solute carrier family 25 member 19	1.6084	6.6617	0.0035763
ERBB3	erb-b2 receptor tyrosine kinase 3	1.6131	5.5599	0.011096
SLC44A3	solute carrier family 44 member 3	1.6393	7.3163	0.044877
RNU1-18P	"RNA, U1 small nuclear 18, pseudogene"	1.6563	5.242	0.014933
ACBD7	acyl-CoA binding domain containing 7	1.6781	5.417	0.031294
ARHGAP42	Rho GTPase activating protein 42	1.7009	7.4096	0.0077782
PLCB4	phospholipase C beta 4	1.7147	8.0638	0.049116
STS	steroid sulfatase	1.7704	8.3111	0.0030569
USP2	ubiquitin specific peptidase 2	1.805	6.1006	0.0045796
LYPLAL1	lysophospholipase like 1	1.8483	7.7959	0.021889
LBH	LBH regulator of WNT signaling pathway	1.8713	8.3898	0.0037299
ANKDD1B	ankyrin repeat and death domain containing 1B	1.9351	5.217	0.012344
AZGP1	"alpha-2-glycoprotein 1, zinc-binding"	2.0043	4.6324	0.0052334
OPCML	opioid binding protein/cell adhesion molecule like	2.0111	4.6977	3.04E-05
CLDN1	claudin 1	2.0664	7.4592	0.0428
CES1P1	carboxylesterase 1 pseudogene 1	2.1004	5.7366	0.0031556
PTCH1	patched 1	2.1348	8.2987	0.011055
CIT	citron rho-interacting serine/threonine kinase	2.3074	6.9864	0.029145
HOMER1	homer scaffold protein 1	2.4677	5.9796	5.59E-06

LMOD1	leiomodoin 1	2.5955	7.5072	0.016248
SERPINA3	serpin family A member 3	2.9497	8.1204	0.028297
SCUBE1	“signal peptide, CUB domain and EGF like domain containing 1”	2.9602	8.0574	0.022483
ECEL1	endothelin converting enzyme like 1	3.0393	7.0535	0.035101
CNTNAP4	contactin associated protein family member 4	3.0562	5.4885	0.013755
PLCXD3	phosphatidylinositol specific phospholipase C X domain containing 3	3.0615	4.7827	0.033297
MGC32805	uncharacterized LOC153163	3.0955	3.9693	2.61E-06
CYP4B1	cytochrome P450 family 4 subfamily B member 1	3.3679	8.7787	0.037478
FAT3	FAT atypical cadherin 3	3.3808	5.6016	0.0025503
TDRD1	tudor domain containing 1	3.5109	4.1305	0.006085
CLIC5	chloride intracellular channel 5	3.7425	7.3253	0.011995
VEPH1	ventricular zone expressed PH domain containing 1	4.5856	4.762	8.28E-06

**Supplementary table 1. Differentially expressed genes between affected and 22 unaffected meningioma cases.**

cauterization, which may be facilitated lymphangiogenesis and dilatation of existing channels<sup>(2)</sup>. Unfortunately, a limitation of this study was related to sample size. Although more brain tumor patients with a history of scalp thermal cauterization are desirable to have included in this study, to confirm the outcomes further, it is challenging to obtain cases with such detailed history, especially in relation to scalp thermal cauterization of childhood. However, we propose that it is necessary to publicize such cases, and perhaps by doing so, more cases are encouraged to be revealed, especially in the Middle East.

In modern medicine, the effect of thermal therapy on human tissue is still under investigation. Storm and coworkers described a magnetic loop applicator for this kind of thermal treatment in human patients<sup>(18)</sup>. It can produce selective heating on either the tumor or brain tissue based on known physical laws. The microwave energy used in this thermal process may be coupled into the tissue by a radiator placed several centimeters above the tissue<sup>(7)</sup>. However, the waves are relatively challenging to focus on, especially on deeper lesions<sup>(13)</sup>. They are entirely different from ionizing radiation used in the treatment of some brain tumors. The radiofrequency current from ionizing radiation is more effective than the microwave thermal energy in producing deep tissue heating<sup>(15)</sup>. If they are located a few centimeters from the skin, the radiofrequency field is much more uniform, and the heat is more uniformly distributed<sup>(15)</sup>. They induce chemical changes with potential biological damage to cellular function. The main event, which initiates damage caused by radiation, breaks in one or both strands of the DNA helix in cells, resulting in cell death, damage

to chromosomes, or mutations. A high dose of ionizing radiation showed a statistically significant increased risk for meningioma, especially at a young age<sup>(3)</sup>.

The association of heat and neoplasia development has never been discussed in detail in the literature, probably because the microwave's thermal energy theoretically does not cause potential biological changes to the cells compared to radiation. However, based on our cases, we have different suggestions that could explain a possible relationship between thermal injury and neoplasia. The cauterization's thermal waves could have crossed the bone and heated the underlying tissue through a process called protein denaturation<sup>(14)</sup>. The stress response initiated by the denatured proteins breaks the double-stranded DNA into single strands<sup>(10)</sup>. The unraveled protein strands stick together, forming an aggregate or network<sup>(14)</sup>. DNA-encoding stress proteins may exhibit cellular mutations, which can change the mitotic division. Over a long-standing period, this change may cause an abnormal cellular growth pattern that leads to unregulated proliferation of these cells and tumor formation. However, these thermal waves helped to initiate or promote tumor growth.

Tissue blood perfusion and the amount of heating exposure play an essential role in this physical process. When tumor perfusion is equal to normal tissue perfusion, there is virtually no selective heating of the tumor. When tumor perfusion is less than usual tissue perfusion, tumor heating is improved<sup>(8)</sup>. Hence, tumors with relatively poor blood flow are more easily heated than tumors with blood flow equal to that in surrounding healthy tissues. This causal relationship could also be applied to healthy tissue

when it is exposed to thermal waves. Reduced blood flow in tumors during heat therapy has essential biochemical and thermal effects. Hypoxia and the resultant anaerobic metabolism and local acidosis make the tumor tissue in the heated region more vulnerable to thermal injury. This phenomenon has been shown quite clearly both *in vitro* and *in vivo* <sup>(12)</sup>.

Microarray expression analysis provided some unique biofunctional insights into genes and pathways related to the affected meningiomas. It is not unusual to use a publicly available gene expression database to analyze a particular factor's effects. Indeed, the bioinformatics field is compacted with meta-analysis data and reviews that apply similar methods. However, no database is currently available, including brain tumor patients' history and habits, particularly in relation to scalp thermal cautery. In our research, the novelty is related to using DNA retrieved from meningioma with a known history of scalp thermal cautery while focusing particularly on infectious-related gene expression. No other cases in the literature provides such analysis.

DNAJC15 is a co-chaperone for HSP70 and was the most significantly deregulated gene. Epigenetic inactivation of the DNAJC15 has been detected in a number of brain tumor types indicating a possible role in tumorigenesis of these tumors (16). Expression of DNAJC15 may also be regulated by binding to a pro-inflammatory transcription factor. VEPH1 is an adaptor protein implicated in several signaling pathways and neuronal cell differentiation in mammals <sup>(4, 17)</sup>. Aberrant expression of VEPH1 has been observed in different types of cancers and cancer cell models.

Although the function of the long non-coding RNA (lncRNA) MGC32805 in normal tissues and malignancies has not been explored in detail, upregulation of lncRNA has been found in recurrent tumors compared to primary gliomas <sup>(6, 11)</sup>. The scaffolding protein HOMER1 is expressed at high levels in brain and muscle tissues and is implicated in Ca<sup>2+</sup> transport and signaling. In inflammatory astrocytes, the HOMER1 splice variant is upregulated and constitutes a possible protective mechanism for adjacent cells by limiting toxic glutamatergic gliotransmission <sup>(5)</sup>. The enriched pathway analysis revealed significant signaling components associated with essential cellular functions and processes related to cell projection morphogenesis, synaptic transmission, and brain development. The pathways may reflect the benign features of the affected meningiomas. The DisGeNET pathway analysis displayed significant signaling components associated with tumor progression, viral infection and other conditions. Notably, the HPV infection pathway points to a feasible projection that an oncogenic and inflammatory viral infection

related to the thermal cautery and dura fibrosis promoted meningioma development.

We suggest a possible correlation between the traditional cautery performed during childhood in our two patients and meningioma development based on the extensive and unusual scalp and dura fibrosis. But to date, we have no clear evidence to say that exposure to thermal cautery is a potential factor in developing neoplasia. Substantial evidence came from one of the well-known studies of ionizing radiation and meningioma risk in Israel between 1948 and 1960. Interestingly, meningioma developed in less than 1% of individuals who received radiotherapy, supporting the idea that other factors (environmental, lifestyle, and genetic) modify tumorigenesis after low-dose irradiation <sup>(20)</sup>. Some researchers examined the relationship between specific genetic variants and meningioma risk, focusing on genes involved in DNA repair, cell cycle regulation, detoxification, and hormone metabolic pathways. One of these recent studies showed a relationship between ionizing radiation and genetic mutation (Excision repair core complex-2) associated with DNA repair damage in some meningiomas <sup>(20)</sup>. These studies may explain that heat injury could be a potential factor in cellular damage to developing neoplastic cells. Alternatively, skin cautery procedure may provide an opportunity for oncoviruses to infect affected sites, and thus in time, contribute to the development of meningioma.

## Conclusion

The association of the traditional skin thermal cautery and the development of underlying neoplasia has neither been explored nor theoretically proven in the literature. Further studies and research are required to confirm our innovative hypothesis. We propose that thermal injury might speed growing any underlying tumor with reduced blood flow. It also could trigger stress injury-mediated by protein denaturation, DNA damage, cellular dysfunction, oncoviral infections, which may initiate tumorigenesis. Our report aimed to raise the awareness of possible remote complications of thermal cautery and call for further advanced studies and research to support this hypothesis.

## Acknowledgment:

Not applicable

## Funding:

We do not have any relationship with the manufacturers and have not received any grant from them.

### Competing interest:

There is no financial relationship that might lead to a conflict of interest in relation to the manuscript.

### Ethics approval and consent to participate:

This work was approved by the Ethical Board of King Abdulaziz University Hospital, board registration number at the National Committee of Bio. and Med. Ethics is HA-02-J-008 and Project Reference No. 710-19. According to the Declaration of Helsinki, a signed informed consent form was obtained for each donated tumor sample.

### Availability of data and materials:

The datasets used and analyzed during the current study are available from the corresponding author on reasonable request.

### References

1. Abou-Elhamd k-E. Kaiy as traditional therapy for pain: Is it helpful or a myth? *The Journal of Laryngology & Otology* 2009;123:566-568.
2. Al-Lawati T, Mehdi I, Al Bahrani B, Al-Harsi K, Rahbi S, Varvaras D. Does Alternative and Traditional WASAM (Local cautery) Therapy Facilitate an Early and More Extensive Loco- regional Metastasis of Breast Cancer? *gulf journal of oncology, The* 2016:11-16.
3. Brenner AV, Sugiyama H, Preston DL, Sakata R, French B, Sadakane A, et al. Radiation risk of central nervous system tumors in the Life Span Study of atomic bomb survivors, 1958-2009. *European journal of epidemiology* 2020;35(6):591-600.
4. Brown TJ, Kollara A, Shathasivam P, Ringuette MJ. Ventricular Zone Expressed PH Domain Containing 1 (VEPH1): an adaptor protein capable of modulating multiple signaling transduction pathways during normal and pathological development. *Cell Communication and Signaling* 2019;17(1):116.
5. Buscemi L, Ginet V, Lopatar J, Montana V, Pucci L, Spagnuolo P, et al. Homer1 Scaffold Proteins Govern Ca2+ Dynamics in Normal and Reactive Astrocytes. *Cerebral cortex (New York, NY : 1991)* 2017;27(3):2365-2384.
6. Chen Y, Wu JJ, Lin XB, Bao Y, Chen ZH, Zhang CR, et al. Differential lncRNA expression profiles in recurrent gliomas compared with primary gliomas identified by microarray analysis. *International journal of clinical and experimental medicine* 2015;8(4):5033-5043.
7. Cuplov V, Pain F, Jan S. Simulation of nanoparticle-mediated near-infrared thermal therapy using GATE. *Biomed Opt Express* 2017;8(3):1665-1681.
8. Elaobda Y, Abu-Hamad M, Treister-Goltzman Y, Peleg R. Traditional Cautery for Medical Treatment Among the Bedouins of Southern Israel. *Journal of immigrant and minority health* 2016;18(1):34-41.
9. Farid MK, El-Mansoury A. Kaiy (traditional cautery) in Benghazi, Libya: complications versus effectiveness. *Pan Afr Med J* 2015;22:98-98.
10. Flint-Richter P, Mandelzweig L, Oberman B, Sadetzki S. Possible interaction between ionizing radiation, smoking, and gender in the causation of meningioma. *Neuro-Oncology* 2011;13(3):345-352.
11. Ghesquieres H, Slager SL, Jardin F, Veron AS, Asmann YW, Maurer MJ, et al. Genome-Wide Association Study of Event-Free Survival in Diffuse Large B-Cell Lymphoma Treated With Immunochemotherapy. *Journal of clinical oncology : official journal of the American Society of Clinical Oncology* 2015;33(33):3930-3937.
12. Gurdita A, Vovko H, Ungrin M. A Simple and Low-Cost Monitoring System to Investigate Environmental Conditions in a Biological Research Laboratory. *PLoS one* 2016;11(1):e0147140.
13. Haemmerich D, Lee FT, Jr. Multiple applicator approaches for radiofrequency and microwave ablation. *International journal of hyperthermia : the official journal of European Society for Hyperthermic Oncology, North American Hyperthermia Group* 2005;21(2):93-106.
14. Ivankov DN, Finkelstein AV. Solution of Levinthal's Paradox and a Physical Theory of Protein Folding Times. *Biomolecules* 2020;10(2):250.
15. Karuppal R, Surendran S, Patinharayil G, Muhammed Fazil VV, Marthya A. It is time for a more cautious approach to surgical diathermy, especially in COVID-19 outbreak: A schematic review. *Journal of orthopaedics* 2020;20:297-300.
16. Lindsey JC, Lusher ME, Strathdee G, Brown R, Gilbertson RJ, Bailey S, et al. Epigenetic inactivation of MCGJ (DNAJD1) in malignant paediatric brain tumours. *International journal of cancer* 2006;118(2):346-352.
17. Muto E, Tabata Y, Taneda T, Aoki Y, Muto A, Arai K, et al. Identification and characterization of Vepf, a novel gene encoding a PH domain-containing protein expressed in the developing central nervous system of vertebrates. *Biochimie* 2004;86(8):523-531.
18. Revia RA, Zhang M. Magnetite nanoparticles for cancer diagnosis, treatment, and treatment monitoring: recent advances. *Materials Today* 2016;19(3):157-168.
19. Schulten H-J, Hussein D, Al-Adwani F, Karim S, Al-Maghrabi J, Al-Sharif M, et al. Microarray Expression Data Identify DCC as a Candidate Gene for Early Meningioma Progression. *PLoS one* 2016;11(4):e0153681.
20. Yamanaka R, Hayano A, Kanayama T. Radiation-Induced Meningiomas: An Exhaustive Review of the Literature. *World neurosurgery* 2017;97:635-644.e638.